ScienceDirect

Minerals Engineering
Volume 201, October 2023, 108239

Evaluation of a novel electrode design for high voltage pulse ore pre-concentration

Daniel Lay, Fengnian Shi, Christian Antonio

Show more

https://doi.org/10.1016/j.mineng.2023.108239
Get rights and content

Highlights

- High voltage pulse selective breakage using grizzly electrode design was evaluated.
- Synthetic particles and a gold-copper ore were tested.
- Ore pre-concentration can be achieved with the grizzly electrodes.
- Factors affecting grizzly electrode performance and limitations were discussed.

Abstract

High Voltage Pulse (HVP) enabled ore preconcentration has the potential to provide large energy savings and upgrade Run-of-Mine ores. The concept is well established in laboratory settings but is yet to be demonstrated at the throughputs needed for industrial uptake of the technology. To scale up this concept from laboratory batch tests to a continuous operation, a novel grizzly-electrode design that integrates pulse discharges for particle breakage and size-based separation into a single step has been patented. In the initial evaluation of the system, two cylindrical electrode bars were adopted with an experiment design to simulate continuous feeding operation. Synthetic particles and a low-grade gold-copper ore were used for the initial evaluation. The evaluation showed pre-concentration can be achieved. Factors affecting the system performance were identified and limitations of the grizzly electrodes are discussed.

Previous Next

1. Introduction

Mineral extraction is increasingly moving towards lower grade ore bodies (Mudd, 2007, Calvo et al., 2016) which represents a challenge for the mining industry. More energy is required to process lower grade ores, and to produce

comparable amounts of metal, more ore must be processed, which generates more waste. High voltage pulses (HVP) are a potential solution. In a process analogous to a lightning strike, HVPs are used to fragment ore particles.

For size reduction purposes, the theoretical efficiency of HVP treatment has been estimated as 0.04–0.32%, which is comparable to mechanical breakage (0.002–1%) (Bluhm, 2006). A practical comparison between HVP breakage and mechanical comminution (rod mill) at the same specific energy levels was made by Wang et al. (2012). It was found that for the same amount of energy, the rod mill achieved better size reduction. For the HVP device to have reached the size reduction seen by the rod mill, it would have required 2.1 times more energy. Differences in mineral liberation and energy requirements were also identified. When looking at the product size fraction 0–3.35 mm, to achieve similar degrees of >95% liberated material, for lower energy inputs mechanical breakage required 8.9 kWh/t while HVP required 4.8 kWh/t. At higher energy inputs, this trend reversed with mechanical requiring 21.9 kWh/t and HVP requiring 39.0 kWh/t. This was attributed to rod mill producing more fines that were less than the chalcopyrite grain size. Because fines have a negative impact on metal recovery, the ability to recover course liberated minerals with lower HVP energy inputs before further grinding to finer sizes can lead to energy savings. It was also noted that a significant amount of product material was larger than 3.35 mm – further size reduction of this material to get more liberation would not be energy efficient with HVPs. These results demonstrated that HVPs are not efficient when used for size reduction, but benefits arise when mineral liberation is considered.

Improved mineral liberation in HVP-treated products has also been observed by several other researchers (Andres, 1977, Andres and Bialecki, 1986, Usov and Tsukerman, 2002). This is thought to be driven by the preferential development of HVPs around the boundaries of mineral grains that have different electrical properties, such as permittivity. Observations have been made of crack growth occurring along grain boundaries (van der Wielen, 2013, Cho et al., 2016), as well as through mineral grains (Huang et al., 2019). Mezzetti et al. (2018) made use of HVPs to fragment complex ores with fine intermixed polymetallic structures. Breakage was found to occur along grain boundaries in some segments of the analysed products. The processing of such ores with conventional methods requires very high energy inputs.

Recently, a new application of HVP was developed in ore preconcentration and coarse waste rejection. Just as differences in electrical properties within particles are thought to influence mineral liberation by controlling where the HVP develops, so too can differences in electrical properties between particles be utilised. High-grade particles are more likely to be selectively targeted and broken by HVP discharges than low-grade or barren particles. This allows HVPs to be used for ore pre-concentration purposes (Zuo et al., 2015a). The HVP product is further treated by a screen, producing a concentrated stream of high-grade particles in the screen undersize and a low-grade or barren stream in the screen oversize which may be rejected, as shown in Fig. 1. The primary purpose of such a HVP application is not size reduction, but to identify high-grade particles. Further conventional processing is then done on the high-grade stream. Energy inputs of less than 10 kWh/t have been reported for HVP pre-concentration treatment (Zuo et al., 2015a, Zuo et al., 2015b, Huang et al., 2020). Furthermore, in the HVP enabled ore preconcentration application, the HVP-damaged particles are also “pre-weakened”, which leads to energy savings in down-stream comminution (Wang et al., 2011, Voigt et al., 2020). Voigt et al. (2020) reported improvements in liberation for some coarse size fractions when HVP-treated products were then subjected to further mechanical treatment.

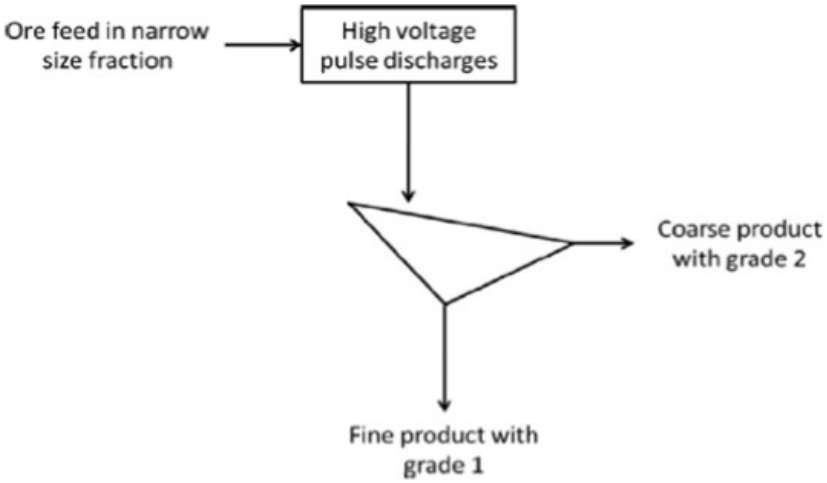

Download : Download high-res image (73KB)

Download : Download full-size image

Fig. 1. Two-step process of pre-concentration using HVPs (Zuo et al. 2015a).

In HVP applications, electrode configurations exert a significant impact on their disintegration performance and energy efficiency. Andres et al. (2001) theoretically investigated energy efficiencies of point-point, point-plane, plane-plane (parallel and angled) electrode configurations. The point-point and point-plane configurations were shown to have the lowest energy losses, with the point-plane option being convenient for processing samples. Usov and Tsukerman (2008) considered the point-plane configuration optimum because of its electric field distribution. This did not consider selectivity. Shi et al. (2013) conducted tests with a SelFrag Lab Unit (point-plane electrode). Three ore particles of 26.5–45 mm were placed in the processing vessel, one directly under the electrode and the other two on the edge. After three pulses were discharged, the centre particle was broken, and the edge particles remained intact or had minor chipping damage. X-ray Tomography found that no cracks or micro-cracks were generated in the unbroken edge particles. This test demonstrated that for a point-plane electrode configuration, particle location in the processing zone affects the selective targeting and pre-weakening results.

Zuo et al. (2015b) compared HVP breakage between a selFrag Lab Unit (point-plane electrode) and a pilot scale Pre-Weakening Test Station (PWTS) also built by SELFRAG (plane-plane electrode). At the same operating conditions the PWTS Unit performed better in terms of body breakage probability and product fineness for two out of the three ores tested. For the third ore tested, the Lab Unit performed better, including in terms of pre-weakening. The differences in performance were thought to be due to the different processing zones. In the PWTS Unit, a disc electrode was used above a conveyor belt (in these tests kept stationary), while in the Lab Unit, a point electrode was used above a grounded plate electrode. The PWTS disc-configuration produced a more uniform electric field. The Lab Unit by contrast, with its tip electrode, strongly concentrated the electric field in its immediate vicinity. It was thought that the chance of a particle serving as the initiation point in the more spread out and uniform electric field of the PWTS was greater than in the smaller more concentrated field of the Lab Unit. This comparison was made with single particle tests. It remains to be seen how this effect would manifest itself with multiple particles. It should also be noted that this effect appears to be ore-dependent. These electrode designs all require the discharge to develop through some distance of water before entering the target particle, increasing energy losses. If used for pre-concentration, they would also involve two steps, with HVP discharges being applied first, and separation taking place secondly, as shown in Fig. 1. An alternative design is the grizzly electrodes, patented by Shi and Manlapig (2018), and illustrated in Fig. 2.

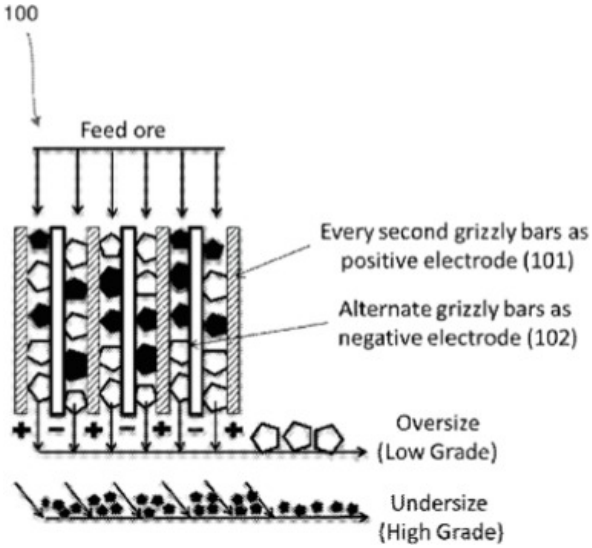

Download : Download high-res image (177KB)

Download : Download full-size image

Fig. 2. Grizzly electrodes schematic (Shi and Manlapig, 2018).

Particles enter the grizzly electrodes, which are inclined, and move from one end to the other. High-grade particles are selectively targeted, break, and fall through the electrodes, creating a high-grade undersize stream; whilst low-grade or barren particles travel to the end of the electrodes relatively undamaged. This approach incorporates point-to-point contact between the high voltage electrode, particle being broken, and the ground electrode, and combines particle breakage and size-based separation into a single step. The grizzly electrode concept was patented in 2018 but has not to date been experimentally verified. This paper aims to evaluate the grizzly electrode processing system with three objectives: 1) to assess its selectivity of breakage; 2) determine energy input ranges for different grades of feed; and 3) to assess its efficacy for ore pre-concentration.

2. Experimental

2.1. Material

Three materials were used to evaluate the grizzly electrodes.

2.1.1. Synthetic particles

Synthetic particles were fabricated to enable control of the “grade” of the particles. They also enable selectivity to be instantly assessed without the need for assaying. Synthetic particles have previously been used in HVP work, for example (Zuo et al., 2014), to reduce any variance that a mineralised ore sample may have introduced by providing precise control over particle shape, size, and mineralisation. The synthetic particles were made from high-strength grout. The procedure for their construction is detailed in (Huang, 2019). The synthetic particles were cylindrical with a height and diameter of 20 mm and an average mass of 13.6 g. The A*b value of the particles was 46, indicating a medium competence. Two sets of particles were made. The first contained a segment of copper wire, 4 mm long and 2 mm in diameter, inserted into the middle of the particle before the grout had set. This simulated a high-grade particle. The copper wire represented 0.8% of the total mass of the high-grade synthetic particle. A second set of fully-grout particles (no copper wire) were constructed to simulate barren particles.

2.1.2. Gold-copper ore

The gold-copper ore used was from New South Wales, Australia. It is a porphyry gold-copper ore with mineralisation occurring as quartz veins, sheeted quartz sulphide veins, and stockworks. The principal copper sulphide minerals are chalcopyrite and bornite. The sample was received in several drums in size fractions 80–150 mm and 150–300 mm. These were crushed with a jaw-crusher until passing 45 mm and separated into desired size fractions using a Gilson screen. For this work, the size fractions used were 19–22.4 mm and 22.4–26.5 mm.

Electrical properties of copper, and the copper and gangue related minerals in the gold-copper ore, are presented in Table 1. Higher conductivity and permittivity values are thought to have higher chances of being selectively targeted by HVP discharges.

Table 1. Electrical properties of various minerals (Olhoeft 1979).

Material	Conductivity dc (S/m)	Permittivity at 1 MHz (F/m)
Copper	$5.9*10^{7}$	>81
Chalcopyrite	1000	>81
Bornite	1000	8.13
Quartz	$2.6*10^{-12}$	4.9

The copper grade by mass distribution for the 19–22.4 mm sample was calculated by individually pulverising and assaying each particle in a representative sub-sample consisting of over 100 particles. After ordering each of the particles from lowest to highest copper grade, the grades associated with different percentages of the sub-sample feed mass were calculated, as shown in Table 2. The lowest grade particles representing 10% of the feed mass have a copper grade range of 0.00–0.01 %, for example.

Table 2. Copper grade distribution by mass for 19 – 22.4 mm size fraction using individual particle assaying.

Incremental mass (%)	Grade range (%Cu)
0–10	0.00–0.01
10–20	0.01–0.02
20–30	0.02–0.04
30–40	0.04–0.08
40–50	0.08–0.12
50–60	0.12–0.17
60–70	0.17–0.25
70–80	0.26–0.43
80–90	0.46–0.63
90–100	0.64–1.32

2.1.3. Microwave-sorted gold-copper ore

Ore grade effects on selectivity were investigated by sorting particles into different grades using microwave processing and infrared thermography (MW/IR) of a gold-copper ore sample. The MW/IR technique has been previously used as a proxy to determine ore grades (Batchelor et al., 2016).

MW/IR-characterisation was only performed on the 22.4–26.5 mm size fraction. Roughly 190 g batches were processed with a microwave oven (Sharp Carousel 1200W). Batches were treated for 12 s (one full revolution on the microwave tray) after which the surface temperature was measured using a hand-held thermal camera as shown in Fig. 3. Tests were conducted at room temperature (25 °C). Particles were sorted into temperature groupings. Random particles from each grouping were then collected, pulverised, and assayed to determine copper and gold content. Fig. 4. shows a roughly linear relationship between surface temperature and copper grade. The primary metal of interest was copper. The 30 °C point in Fig. 4 was based on 13 randomly selected particles, which were combined, crushed, and pulverised for a single assay. All other data points were based on the assay of seven combined particles each.

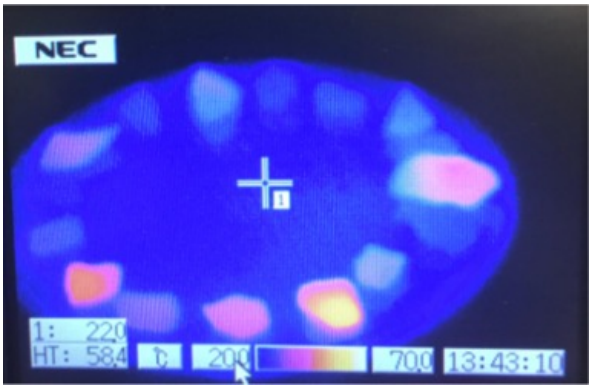

Download : Download high-res image (134KB)
Download : Download full-size image

Fig. 3. Thermal camera image of microwave processed gold-copper ore.

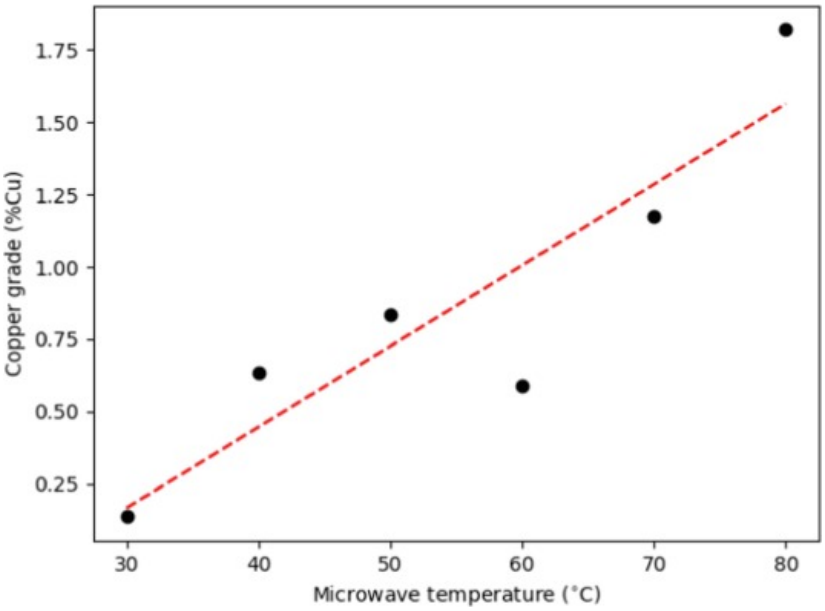

Download : Download high-res image (91KB)
Download : Download full-size image

Fig. 4. Relationship between post-microwave surface temperature and ore-grade.

Roughly 70% of the feed reported minimal or no increase in surface temperature after microwave treatment, as indicated in Table 3. Based on previous experience with this ore, treating 70% of the feed as waste due to low ore grades is not accurate. The<30°C group should not be regarded as waste and likely still contains some degree of valuable copper. This grouping could not be split further into smaller temperature groupings. The estimated copper grades for different temperature groups are presented in Table 3.

Table 3. Estimated copper grades and mass proportion of feed for different temperature groups.

Temperature group (°C)	Copper grade (% Cu)	Mass proportion (%)
<30	0.1	69.9
40	0.4	15.7
50–60	0.8	7.8
70 - >80	1.4	6.6

2.2. Equipment

Samples were subjected to HVP discharges using a grizzly electrode bar assembly constructed at the JKMRC, connected to a HVP generator built by Huazhong University of Science and Technology (HUST). The generator uses a pulse transformer to output high voltages. The high-voltage and the ground terminals from the HUST generator (Fig. 5) were connected to the grizzly electrode bars, Fig. 6. The electrodes were made from stainless steel. Insulating guiderails were used in some experiments to prevent particles jumping off the electrodes. During operation, the grizzly electrodes are submerged in water. Charging voltage increments (1, 2, 3, 4, 5 kV) are set using the control computer in the primary circuit, which are then transformed to higher output voltages at the processing zone. The voltage pulse rise time is roughly 120 ns. A single discharge contains roughly 60 J. If the energy required by particles to pass the grizzly electrodes is less than the discharge energy this risks energy losses as a less powerful discharge would have been sufficient. During the preliminary and main test work, several discharges were required for most particles to pass the grizzly electrodes. While discharges can be applied at up to 5 Hz, all tests were effectively performed as single discharges, due to time requirements for saving waveforms and the need to ground the system and inspect samples between discharges.

Download : Download high-res image (145KB)
Download : Download full-size image

Fig. 5. HUST generator and output terminals.

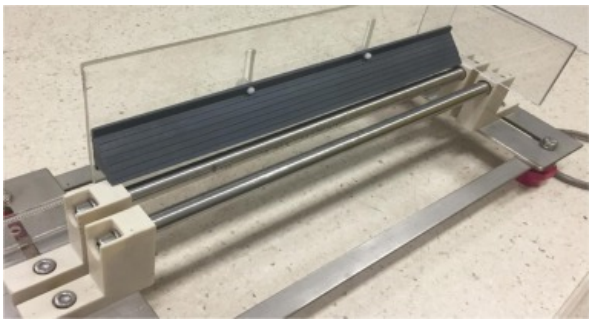

Download : Download high-res image (168KB)
Download : Download full-size image

Fig. 6. Grizzly electrodes with guiderail.

Voltage and current signals were recorded using voltage and current probes and an oscilloscope. The waveforms were saved to a USB and later processed on a computer to extract energy input and other waveform properties. The spark energy was calculated following the procedure outlined in (Han et al., 2015).

$$E_{spark} = R \int_{t_d}^{t_\infty} i^2 \, (dt)$$

where R is the spark resistance, t_d is the discharge start time, t_∞ is the discharge end time, and $i(t)$ is the recorded current signal. These waveform properties are illustrated in Fig. 7.

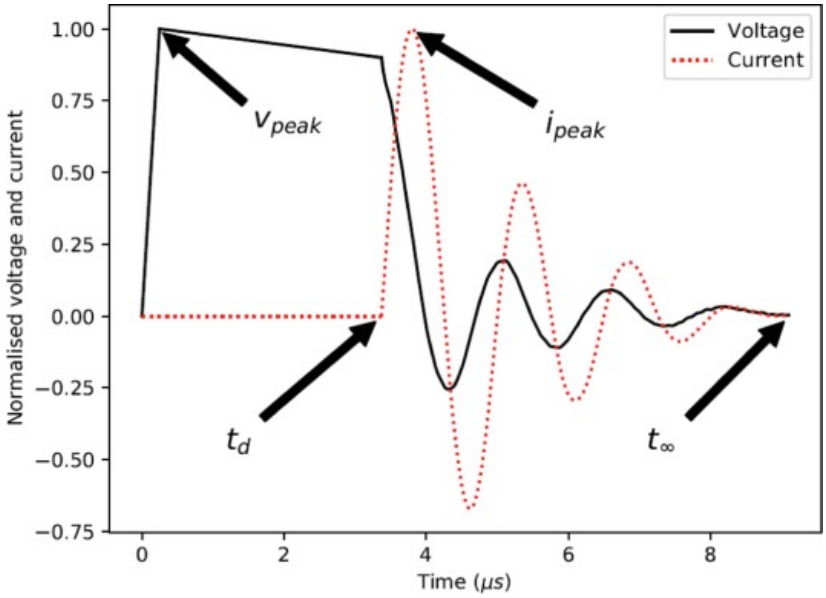

Download : Download high-res image (167KB)

Download : Download full-size image

Fig. 7. Illustration of selected waveform properties for theoretical voltage and current signals.

The voltage probe was a North Star PVM-100. Voltages signals which exceed the recording limit are possible depending on experimental conditions. To account for this, a liquid resistor (voltage divider) was used to reduce the input voltage to the voltage probe. The liquid resistor consisted of two sections filled with copper sulphate solution. The smaller section was one third of the total length of the liquid resistor. The copper sulphate solution had a conductivity of 1.4 μ S/cm. The true voltage was then determined by accounting for the liquid resistor voltage drop. The current probe was a Pearson 1330. The oscilloscope used was a Tektronix DPO2024B.

2.3. Testing procedure

The grizzly electrodes were evaluated in several steps. Initially, synthetic particles and then a gold-copper ore that had been sorted into different grades were used to determine if selectivity could be achieved with synthetic and real ores. Next, the sorted gold-copper ore was used to assess what energy input ranges were necessary for particles to not just be selectively damaged, but to be damaged enough to pass the grizzly electrodes, and what effect ore grade had on this. In the final stage of testing, an unsorted gold-copper ore was processed using the settings established by the previous steps to assess ore preconcentration performance.

2.3.1. Grizzly electrode setting test with synthetic particles

It was first necessary to establish if the grizzly electrodes could selectively target high-grade particles, and if they could, what influenced this selectivity. This was evaluated using barren (pure grout) and copper synthetic particles (grout+embedded copper wire).

Two-particle tests were performed with one barren synthetic particle and one copper-embedded synthetic particle. A single discharge was applied and the particles were then inspected for signs of damage. If a particle showed any damage it was treated as that particle having been targeted. The possible responses were copper particle targeted, barren particle targeted, or both particles targeted. If neither of the particles showed any damage, another discharge was applied. A charging voltage of 4kV was used. The electrode gap used was 20mm, the maximum gap possible for the synthetic particles. The electrode gap was taken as the shortest distance between the edges of the cylindrical electrodes.

Fig. 8 shows the three different positions along the grizzly electrodes which were tested, position 1, 2, and 3. Synthetic particle pairs were placed at two out of these three positions. For example, both particles at position 1 (C1-B1), copper particle at position 1 and barren particle at position 2 (C1-B2), C1-B3, C2-B1, C2-B2, C2-B3, C3-B1, C3-B2, C3-B3. Five repeat tests were performed at each position. When positioned next to each other, the two particles were not touching.

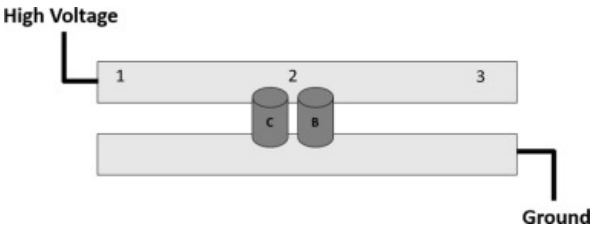

Download : Download high-res image (30KB)

Download : Download full-size image

Fig. 8. Synthetic particle positions on the grizzly electrodes. A copper-embedded (C) and barren (B) synthetic particle pair are shown at position 2 (C2-B2).

2.3.2. Selective breakage test with MW/IR-sorted gold-copper ore

Tests were performed to check if grade selectivity also occurred for a real ore sample. Selectivity was assessed using a gold-copper ore that had been split into different grades, size fraction 22.4–26.5 mm.

Three temperature groups (ore grades) were investigated. Particles pairs of one gold-copper particle and one basalt particle were subjected to a single discharge. Basalt was used to represent a barren particle. The primary response assessed was selectivity. If the gold-copper particle was damaged but not the basalt particle, this was recorded as the gold-copper particle being selectively targeted. Energy input was also recorded.

The particles were placed in a central position on the grizzly electrodes, as shown in Fig. 9. This was due to the minimal differences in selectivity noted in the synthetic particle experiments at different positions on the grizzly electrodes and to simplify the experimental design. A single electrode gap (15 mm) was also used. This was the largest electrode gap that could be used with this size fraction. Other test settings are shown in Table 4.

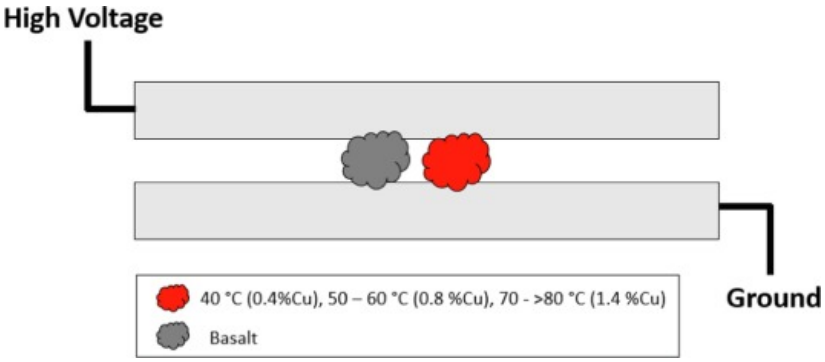

Download : Download high-res image (73KB)

Download : Download full-size image

Fig. 9. Particle positions for selective breakage tests with MW/IR-sorted ore.

Table 4. Test settings for selective breakage test with MW/IR-sorted ore.

Run	Temperature group (°C) paired with basalt
1	40 (0.4% Cu)
2	50–60 (0.8 % Cu)
3	70 - >80 (1.4% Cu)

Runs 1 and 3 consisted of 10 batch tests, repeated once for a total of 20 batch tests. Run 2 consisted of 10 batch tests, repeated five times for a total of 50 batch tests. The run 2 temperature grouping was roughly in-between runs 1 and 3.

2.3.3. Energy range test

The selectivity results for the synthetic particle tests and MW/IR-sorted tests provided information about the selectivity of the grizzly electrodes based on instances of damage being done to particles, but not on whether these damaged particles could pass the grizzly electrodes. For the grizzly electrodes to work for pre-concentration purposes, a balance must be struck between applying too little energy (no particle breakage, no particles passing the grizzly electrodes), and too much energy (all particles passing the grizzly electrodes). The energy efficiency tests investigated the energy input ranges required to selectively break high-grade particles with a minimal damage on low-grade particles when passing the grizzly electrode bars, using MW/IR sorted gold-copper ore.

Basalt and a 50–60 °C gold-copper sample were subjected to single-particle tests to determine how many discharges were required to cause them to pass the grizzly electrodes. The case of the single 50–60 °C sample having discharges applied until it breaks represents an ideal case, being equivalent to a mineralised particle being repeatedly targeted until it passes the grizzly electrodes. From Table 3, roughly 70% of the feed mass reported minimal or no heating after MW/IR treatment (<30 °C). The 40 °C group was thought to be too close to this to represent a significant grade difference, hence the 50–60 °C was chosen to represent a high-grade gold-copper particle. There were also more samples available in this grouping than others. Basalt was used to represent a completely barren particle. The single basalt particle case represents the worst-case scenario, with the low-grade or barren particle being repeatedly targeted. The test settings are shown in Table 5. Discharges were applied until there were 20 breakage events (passing the grizzly bars) for the high-grade samples. A charging voltage of 4 kV was used.

Table 5. Test conditions for single particle tests of the MW/IR-sorted gold-copper ore, processed until passing the grizzly electrodes.

Variable	Setting
Number of discharges	Until 20 high-grade passing
Charging voltage	4 kV
Electrode gap	15 mm
Size fraction	22.4–26.5 mm
Gold-copper temperature group	50–60 °C
Position on grizzly electrodes	Central

To simulate realistic operation of the grizzly electrodes, another set of tests with multiple particles and simulated movement through the processing zone were performed. As illustrated in Fig. 10, six particles were placed on the grizzly electrodes, and a single discharge was applied. The particles were then inspected. If no particles had passed the grizzly electrodes, then they would all be moved one position to the right, for example position A→position B, B→C,.., F→A. If a particle passed the grizzly electrodes, then that particle was replaced with a fresh particle in the same position. All particles were then moved along one position to the right. Another discharge was then applied and the process was repeated. Test settings are shown in Table 6. Numbers were drawn onto the rocks with a permanent marker for ease of identification. Six particles represent the highest amount of particles for this size fraction which could be fit on the grizzly electrodes and still identify rocks after movement from discharges. The responses recorded were energy input, the number of discharges input, and selectivity.

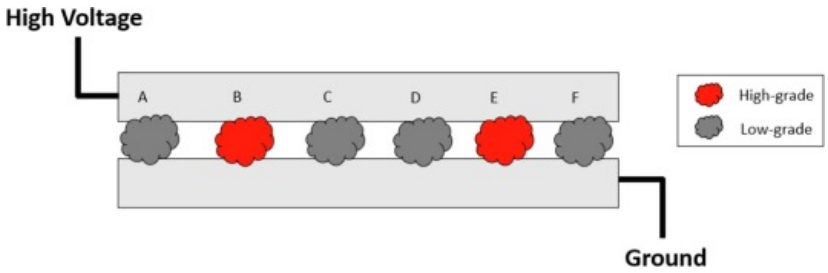

Download : Download high-res image (61KB)

Download : Download full-size image

Fig. 10. Simulated particle positions in dynamic operation using MW/IR-sorted gold-copper ore and basalt.

Table 6. Simulated dynamic operation test settings with MW/IR-sorted particles.

Variable	Setting
Number of discharges	Until target number of high-grade particles broken
Charging voltage	4 kV
Electrode gap	15 mm
Size fraction	22.4–26.5 mm
Number of particles on grizzly electrodes	6
Split of low- and high-grade particles	2/6 high-grade, 4/6 low-grade

Three separate dynamic tests were performed, looking at different ore grade combinations:

1. Gold-copper<30 °C vs. 50–60 °C (0.1 vs. 0.8 %Cu);
2. Basalt vs. gold-copper 70 - >80 °C (barren vs. 1.4 %Cu);
3. Gold-copper<30 °C vs 70 - >80 °C (0.1 vs. 1.4 %Cu).

Due to sample availability, Tests 2 and 3 were performed with 10 high-grade passing events instead of 20.

The first dynamic test represents a re-construction of the feed grade distribution for the unsorted ore sample with 4/6 (66%)<30 °C particles matching the feed distribution of 70 % < 30 °C in Table 2. The 50–60 °C was chosen for the high-grade particle for the same reasons as outlined for the single particle tests. The second and third tests have larger grade differences than the first and were done to explore the effect of grade differences on selectivity and energy input.

For the multiple particle tests, for each discharge, the position and mass of the particles on the grizzly bars was recorded, and the spark energy was calculated. The spark energy was used with the summed mass of the 6 particles currently on the grizzly bars (including low- and high-grade particles together) to calculate the specific energy input for the 6 particles for each discharge. Even though only one particle may be broken, the mass of six was used in the calculations as all rocks were equally exposed. As it was recorded when every particle was added or removed (passing the grizzly bars), this allowed the total specific energy input for every particle in the test to be calculated by summing the energies that each particular particle received while on the grizzly bars. The average number of discharges or specific energy input for the low- and high-grade particles to pass the grizzly electrodes was then calculated. The masses used were unbroken masses, recorded prior to the tests beginning.

The slot-effect of the grizzly electrodes means that flat, plate-like particles, which when sized on square-slotted sieves may have a size larger than the grizzly electrode gap, can still pass the grizzly electrodes unbroken, resulting in misclassification. Plate-like particles were removed and not tested.

2.3.4. Ore pre-concentration test

An un-sorted (not split into grades using MW/IR) gold-copper ore was processed using settings developed in earlier tests. A range of energy inputs were investigated. The gold-copper ore was processed in simulated dynamic operation (explained below). Test settings are shown in Table 7. A smaller size fraction was used than in the energy efficiency tests due to limited sample availability. The electrode gap was adjusted to 12.5 mm for the smaller size fraction. This maintained a similar ratio between the geometric mean feed size and electrode gap. The electrode gap could be adjusted in 0.5 mm increments. The differences in masses between particles in the 19–22.4 mm and 22.4–26.5 mm size fractions would cause differences in specific energy. Fig. 11 shows ore particles sitting on the grizzly electrodes which did not pass unbroken. A total of 6, 9, 11 and 14 discharges were applied, respectively, to the particles. These energy inputs were based on those established in the energy efficiency tests. By extending them, a range of copper and mass recoveries could be explored, as well as covering any differences in required energy inputs between the different size fractions.

Table 7. Simulated dynamic operation test settings with un-sorted gold-copper ore sample.

Variable	Setting
Total number of particles per test	90
Number of particles on grizzly electrodes	6
Charging voltage	4 kV
Electrode gap	12.5 mm
Size fraction	19–22.4 mm
Target number of discharges per particle	6, 9, 11, 14

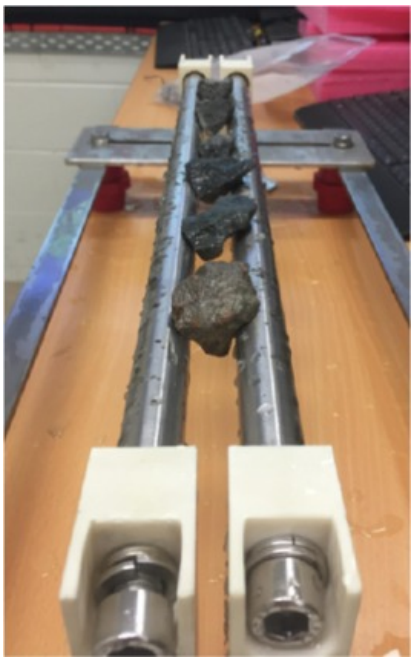

Download : Download high-res image (146KB)
Download : Download full-size image

Fig. 11. Grizzly electrodes with the gold-copper ore sample.

For this test, all particles were fed through the un-powered grizzly electrodes first, and any plate-like particles which passed unbroken were removed. This was roughly 20% of the feed.

Six particles were placed on the grizzly, and dynamic operation of the grizzly electrodes was simulated by incrementally moving the particles along the grizzly electrode after each discharge. A total of 90 particles were processed in each experimental run. Four runs were performed in total to assess variability. Any particles that

remained on the grizzly electrodes (oversize) after the desired number of discharges were removed. The undersize was collected and stored separately. The oversize was then used as the feed for the next round of discharges, and the new undersize collected separately and the process was repeated e.g. the oversize particles from the 1st cycle (6 discharges) were collected and used as the feed of the 2nd cycle. An additional 3 discharges were applied to make up a total 9 discharges for the 2nd cycle products (9 discharges are from the combined cycles 1 and 2). No fresh feed particles were added between cycles. The undersize from 6, 9, 11, and 14 discharges were then dried, pulverised, and assayed. Through back-calculation all required grade information was then obtained for the four different discharge settings. Cumulative mass and copper recovery for each of the discharge settings were then calculated, and from this pre-concentration curves were generated.

The specific energy was calculated and is presented as a cumulative running total, i.e. as the total energy input up to that point, divided by the total mass. For the first cycle, this was the summed cycle 1 spark energy divided by the total mass. For the second cycle it was the summed cycle 1+cycle 2 spark energy divided by the total mass, and so on. The final specific energy input was the total spark energy input for all cycles divided by the total mass.

3. Results and discussion

3.1. Selectivity of breakage

The probabilities of synthetic particles being damaged subjected to one pulse discharge is given in Table 8. The results are presented in the order of percentage of copper-embedded particle broken, barren particle broken, and both particles broken, which sum up to 100%, for all testing positions. 90% confidence intervals are presented, based on binomial proportions, considering each test as a Bernoulli trial.

Table 8. Selectivity of breakage for synthetic particles pairs subjected to one discharge.

Electrode gap (mm)	Copper selectivity (%)	Barren selectivity (%)	Both targeted (%)
20	91.4 (81.2, 97.0)	4.3 (0.8, 13.1)	4.3 (0.8, 13.1)

Slightly higher copper selectivity was noted when the copper particles were at the ends of the grizzly electrodes (positions 1 and 3), but this effect was small.

The synthetic particle experiments demonstrated that the grizzly electrodes can selectively target high-grade copper synthetic particles in the paired tests with barren synthetic particles. To assess the effects of a natural ore with multiple mineral grains randomly distribute within the particles, instead of concentrated at a single copper wire insert, a gold-copper ore was also used to assess the selectivity of breakage.

The selectivity and the effects of ore-grade obtained when using paired tests with one MW/IR sorted gold-copper particle and one basalt are summarised in Table 9. The relationship between selectivity and ore-grade is shown in Fig. 12. The 90% binomial proportion confidence intervals for gold-copper selectivity are presented in Fig. 12.

Table 9. Selective breakage results for MW/IR-sorted paired with basalt tests.

Run	Temperature group (°C) paired with basalt	Gold-copper targeted (%)	Basalt targeted (%)	Both targeted (%)	Specific energy (kWh/t)
1	40 (0.4% Cu)	70	25	5	0.3
2	50–60 (0.8 % Cu)	90	10	0	0.3
3	70 - >80 (1.4% Cu)	85	5	10	0.3

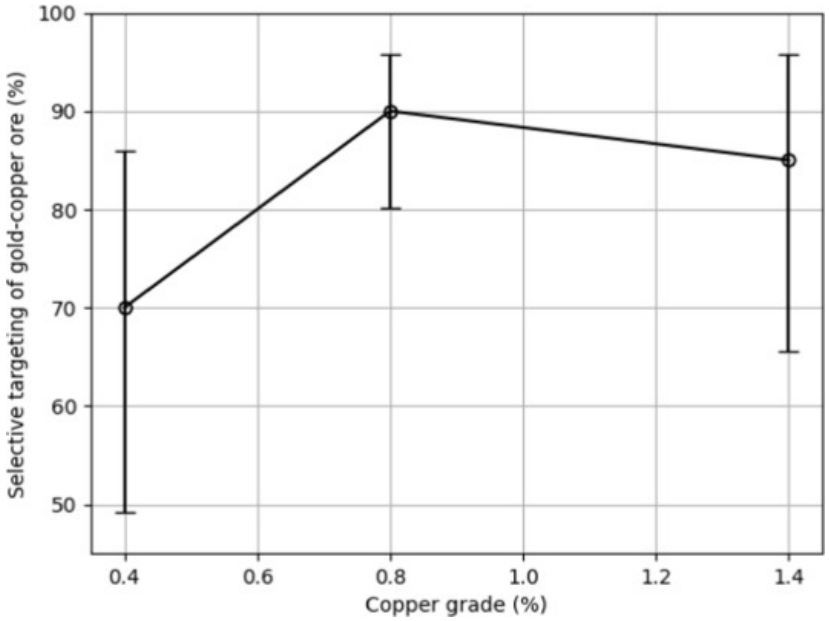

Download : Download high-res image (124KB)

Download : Download full-size image

Fig. 12. Relationship between breakage selectivity and ore grade in the MW/IR-sorted paired-particle with basalt tests.

The results demonstrated that all grades of the gold-copper ore were selectively targeted when paired with basalt. This is attributed to differences in electrical properties between the basalt and the gold-copper samples. The error bars in Fig. 12 are 90% binomial proportion confidence intervals based on considering the tests as Bernoulli trials. Success was defined as the gold-copper particle being selectively targeted, failure was defined as every other outcome (basalt targeted, or both targeted). The larger intervals for 0.4% Cu and 1.4% Cu are due to these being based on a smaller number of tests. Due to the experimental variation, we cannot make any statement about the effect of ore grade on selectivity. The accuracy of the MW/IR-sorting technique in creating the different grade groups likely also contributes to this variability.

The MW/IR-sorting tests demonstrated that the grizzly electrodes can selectively target mineralised particles when treating real ores, like that observed in the synthetic particle tests.

3.2. Energy range

For the single particle tests, Table 10 shows clear differences between the gold-copper ore and basalt. To pass the grizzly electrodes, basalt required an average energy input of 3.3 kWh/t, whereas the gold-copper ore required 1.8 kWh/t. 90% confidence intervals are also shown. The difference is illustrated graphically in Fig. 13 as a cumulative breakage probability plot. An energy input of 2.5 kWh/t would cause roughly 80% of the gold-copper particles to pass the grizzly electrodes, but the same energy input would cause only 50% of the basalt particles to pass. The relative closeness of the two curves is attributed to the non-selectivity of single-particle tests. The pulse energy is forced into the single particle that is in the processing zone. In multiple particle tests, high-grade particles would be preferentially targeted, protecting the barren particles from breakage.

Table 10. Average number of discharges and energy input to pass the grizzly electrodes in single-particle configuration.

Ore sample	Number of discharges to pass grizzly bars	Specific energy (kWh/t)
Basalt	6.5±1.2	3.3±0.7
Gold-copper 50–60°C	3.2±0.7	1.8±0.4

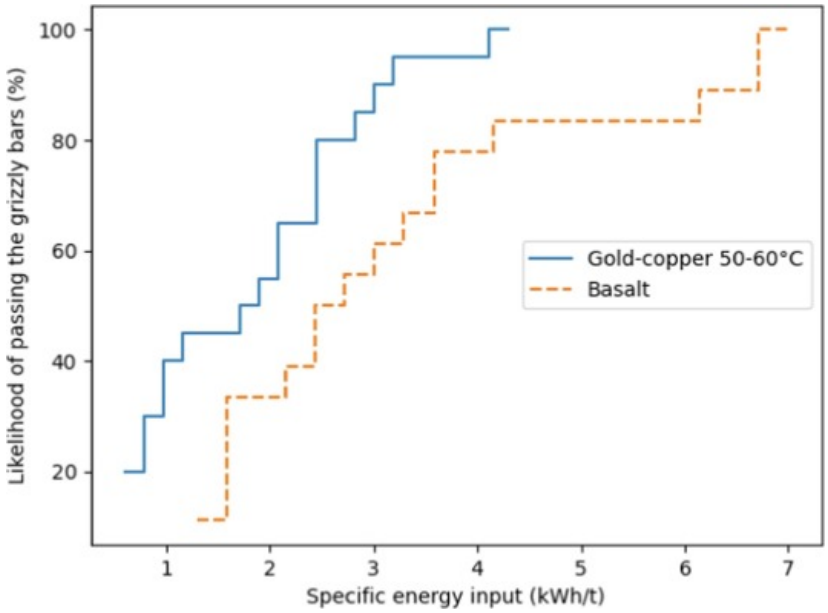

Download : Download high-res image (108KB)

Download : Download full-size image

Fig. 13. Cumulative probability plot vs energy input to pass grizzly electrodes in single particle configuration.

Table 11 summarises the results for the simulated dynamic movement tests with two high-grade and four low-grade particles on the grizzly electrodes simultaneously for each pulse discharge. The testing procedures are described in Section 2.3.3. The 90% confidence intervals are included. In Test 2, one high-grade sample required 33 discharges and 3.2 kWh/t to pass; the next highest was 8 discharges and 0.7 kWh/t. The resultant energy input lower confidence interval has been cut-off at zero. In Test 3, only two low-grade particles broke, resulting in the very large intervals presented, which have also been cut off at zero. An energy input of zero is not realistic. In these cases, only a maximum energy value has been presented in Table 11 in brackets.

Table 11. Average number of discharges and energy input to pass the grizzly electrodes in the simulated dynamic movement tests.

Test	Ore temperature group	Number of discharges to pass grizzly bars	Specific energy input (kWh/t)
Test 1	<30°C (0.1 % Cu)	14.6±5.9	1.9±0.7
	50–60°C (0.8% Cu)	10.7±5.4	1.3±0.6
Test 2	Basalt	No damage	3.9 (no damage)
	70–>80°C (1.4% Cu)	7.0±5.3	0.7 (1.5)
Test 3	<30°C (0.1 % Cu)	11.5 (26.9)	1.3 (3.2)
	70–>80°C (1.4% Cu)	6.9±4.1	0.8±0.5

The experimental variation in Table 11 means we are limited in our ability to differentiate the energy inputs requirements for the different ore grade combinations. The low- and high-grade groups from Tests 1 and 3 cannot be distinguished. Test 2, which represented an exaggerated grade difference did not have any breakage of the basalt, with 100% selective targeting of the high-grade gold-copper ore. The upper energy limit of 1.5 kWh/t may be appropriate in this case. Due to time constraints, and as the original intention of these tests was to provide a range of energy inputs to guide the final pre-concentration tests, no further testing was undertaken.

The variability seen may also be attributed to issues with the MW/IR-sorting process. The average copper grade of the particles reporting to the<30°C temperature group was 0.1% Cu, and these made-up 70% of the feed mass. As shown in the copper grade by mass distribution determined from individual particle assaying, by which particles were ranked from lowest to highest grade (Table 2), the 70% of low-grade particles also averaged 0.1% Cu, but with a range of 0.0–0.25% Cu. The<30°C grouping therefore likely had higher grade particles present, possibly up to 0.25% Cu. Grouping this range of grades together likely contributed to the variability seen in the response. Visually these particles could not be distinguished using surface temperature and the treatment method described in Section 2.1.3. Additional HVP selectivity tests may help to reduce the variability seen, but the initial MW/IR-sorting must be taken into account as well as ore grade is not the only variable affecting the response.

From Test 1, with a grade distribution roughly matching the unsorted feed, an energy input range of 0.7–1.9 kWh/t for the higher-grade particles to pass the grizzly electrodes was identified. For Tests 2 and 3, which represented exaggerated grade-difference cases, this was<1.5 kWh/t.

The energy range tests demonstrated energy input ranges which could be expected. Practically, there is an optimal range of energy input required for the HVP pre-concentration process to be viable. A target range (<1.9 kWh/t) for this has been established, which will be used to guide the preconcentration testing.

3.3. Pre-concentration efficiency

Four repeat tests were conducted using the grizzly electrodes to treat an un-sorted gold-copper ore sample to assess the pre-concentration efficiency. The ore was processed in simulated dynamic operation. The test settings and the procedures are given in Section 2.3.4. Fig. 14 (a) shows the pre-concentration curves plotted as cumulative copper recovery versus cumulative mass recovery to the grizzly undersize product for the four tests, while Fig. 14 (b) presents an expanded view of the pre-concentration curves with marked specific energy input.

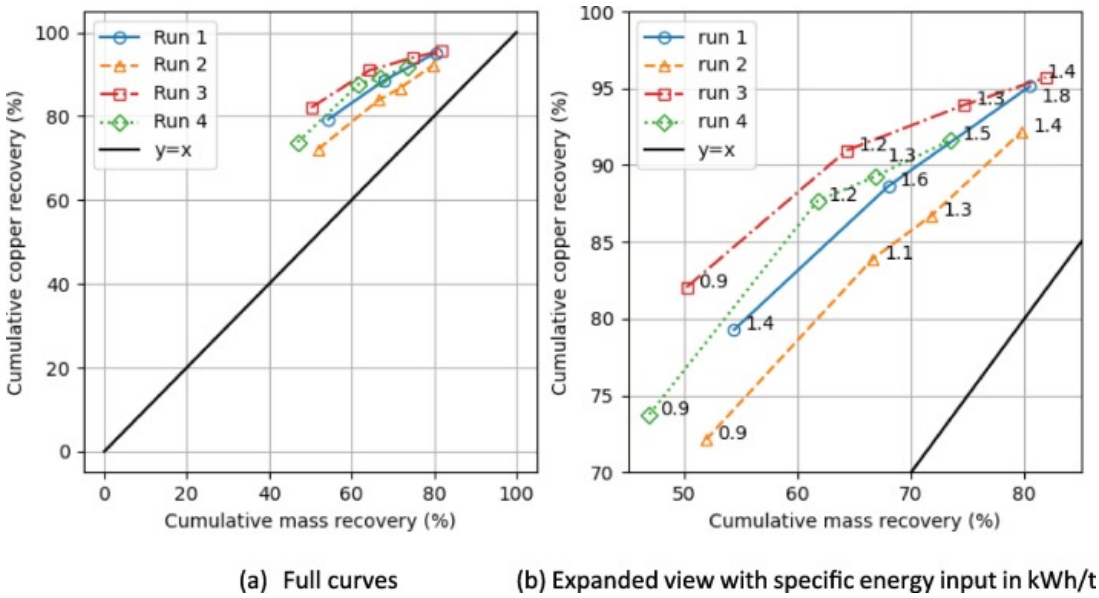

Download : Download high-res image (395KB)

Download : Download full-size image

Fig. 14. Pre-concentration curves for the grizzly electrodes to process an un-sorted gold-copper ore in simulated dynamic operation.

Each point in Fig. 14 represents a single energy input with the leftmost point being the lowest energy setting, and the rightmost the highest. After each energy input (corresponding to 6, 9, 11, and 14 discharges) the undersize products were collected and assayed separately. Taking the average of these yields an energy input of 1.4 kWh/t was required to collect 90% of the copper in the feed while rejecting 30.7% of the mass (recovering 69.3% by mass to the grizzly undersize product).

To assess ore amenability to pre-concentration, a Pre-concentration Indicator (PCI) is introduced (Huang et al., 2020). The PCI is defined as the difference between a nominal metal recovery and the mass yield to concentrate in order to achieve the desired metal recovery. The PCI can be determined from the recovery-mass yield to concentrate curve using a spline function. The nominal metal recovery is often set at 90%. In the above example, the PCI is 20.7% (=90%-69.3%).

Fig. 15 takes the average of the four runs of pre-concentration tests with the grizzly electrodes. The shading represents one standard deviation. The Perfect curve is from the copper heterogeneity curves generated for the same ore sample in the same size, using the copper grade by mass distribution data presented in Table 2. More details about the grade heterogeneity curve can be found elsewhere (Huang et al., 2020). The copper grade heterogeneity curve represents the highest possible separation efficiency that may be achieved and is only dependent on the intrinsic distribution of copper across the over 100 particles selected randomly. The diagonal line refers to a homogeneous material with copper distributed evenly in every particle. An ore with these characteristics would not be amenable for pre-concentration, e.g. 90% copper being recovered from 90% of the mass of the feed particles. The further the test results deviate from this reference line and closer to the Perfect curve, the greater the potential for pre-concentration.

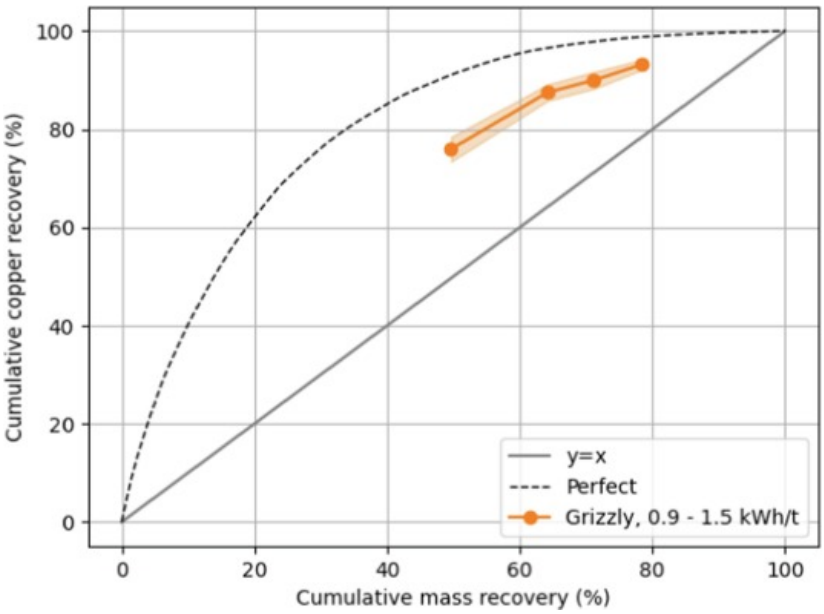

Download : Download high-res image (154KB)

Download : Download full-size image

Fig. 15. Average grizzly electrode pre-concentration performance compared to the perfect separation heterogeneity curve. Shading represents one standard deviation.

This result shows that the grizzly electrodes can perform effective pre-concentration with a real ore sample with less than 2 kWh/t of energy input. A more detailed comparison of the grizzly electrodes as compared to existing HVP electrode designs is left for a separate publication.

The grizzly electrodes were able to recovery 90% of the copper while rejecting 30.7% of the mass. From Table 2, the 30% lowest-grade particles had copper grades ranging from 0 to 0.04%. This suggests that most of the particles which would be expected to be selectively targeted and broken under ideal separation conditions are above this grade range. This represents the ideal case, practically the threshold grade may be higher. The<30°C group in Section 3.2 had an average grade of 0.1 %Cu, with some particles possibly being up to 0.25 %Cu. The particles in this group above the threshold grade value would likely have been selectively targeted, contributing to the variability seen.

Particles on the grizzly electrodes are exposed to the electric field between the electrodes in an approximately uniform fashion, with the electric field shown in Fig. 16 extending along the length of the electrodes. This ensures that, roughly, each particle in the processing zone is given an equal chance to be selectively targeted by the discharge. By processing six particles at once, there is also a greater chance that a higher-grade particle will be present and can be targeted

compared to tests with fewer particles. When high-grade particles are present in the processing zone, the pulse energy is absorbed preferentially by the high-grade particles, which "protects" the low-grade particles in vicinity of the processing zone from being broken, leading to a higher rejection rate for the low-grade particles.

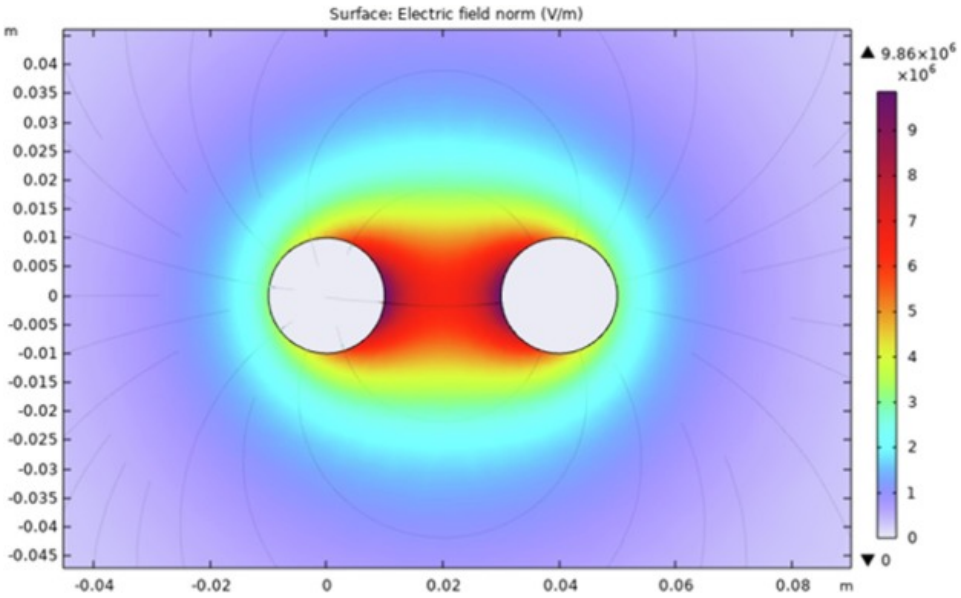

Download : Download high-res image (195KB)

Download : Download full-size image

Fig. 16. Cross sectional view of the grizzly electrodes and the electric field distribution for a voltage of 150 kV.

Experimental limitations have necessitated that certain restrictions be imposed. Firstly, flat rocks that would have passed the grizzly electrodes unbroken have been excluded from the feed, representing 20% of the feed being rejected before being processed with the grizzly electrodes. In practice, this proportion could be pre-screened and treated separately, either using smaller gaps or by a different processing technology. The patent offers the options of HVP treatment in stages, with a smaller electrode gap setting for the second stage to clean the first stage undersize product (Shi and Manlapig, 2018). The issue of particle shape can be resolved with this option. Secondly, simulated dynamic operation of the grizzly electrodes involved placing the particles in designated, evenly spaced locations along the grizzly electrodes for each discharge. In real operation particles would land on top of one another and get bunched up and would not be reorganised into evenly spaced locations. These are areas which should be explored in future work.

4. Conclusions

The operation of a novel electrode design for HVP ore pre-concentration has been demonstrated.

Tests with synthetic particles showed that the grizzly electrodes can perform selective breakage of copper-embedded particles with high selectivity. Similar tests with real ores split into different grades using MW/IR processing showed that selective breakage was also possible with real ores, and the energy inputs required.

Finally, tests with an un-sorted gold-copper ore showed that good pre-concentration performance can be obtained with the grizzly electrodes. With an energy input of 1.4 kWh/t, 30.7% of the mass could be rejected while retaining 90% of the copper for a gold-copper ore. A particle shape effect was noted and is a limitation of the grizzly electrode design.

CRediT authorship contribution statement

Daniel Lay: Conceptualization, Methodology, Software, Validation, Formal analysis, Investigation, Writing – original draft, Visualization. **Fengnian Shi:** Conceptualization, Methodology, Formal analysis, Writing – review & editing, Supervision, Project administration. **Christian Antonio:** Conceptualization, Methodology, Formal analysis, Writing – review & editing, Supervision, Project administration.

Declaration of Competing Interest

The authors declare the following financial interests/personal relationships which may be considered as potential competing interests: Daniel Lay reports financial support was provided by Newcrest Mining Limited. Daniel Lay reports financial support was provided by Newmont Corporation. Daniel Lay reports equipment, drugs, or supplies was provided by Huazhong University of Science and Technology. Frank Shi has patent #2018/232438 issued to Frank Shi.

Acknowledgements

This research was supported by an Australian Government Research Training Program Scholarship. The authors also wish to acknowledge the support of Huazhong University of Science and Technology, Newcrest Mining Limited, and Newmont Corporation.

Special issue articles Recommended articles

Data availability

Data will be made available on request.

References

Andres, 1977 U.T. Andres

Liberation study of apatite-nepheline ore comminuted by penetrating electrical discharges

Int. J. Miner. Process., 4 (1) (1977), pp. 33-38

View PDF View article View in Scopus ↗ Google Scholar ↗

Andres and Bialecki, 1986 U. Andres, R. Bialecki

Liberation of mineral constituents by high-voltage pulses

Powder Technol., 48 (3) (1986), pp. 269-277

View PDF View article View in Scopus ↗ Google Scholar ↗

Andres et al., 2001 U. Andres, I. Timoshkin, M. Soloviev

Energy consumption and liberation of minerals in explosive electrical breakdown of ores

Min. Process. Extractive Metall., 110 (3) (2001), pp. 149-157

CrossRef ↗ Google Scholar ↗

Batchelor et al., 2016 A.R. Batchelor, R.S. Ferrari-John, J. Katrib, O. Udoudo, D.A. Jones, C. Dodds, S.W. Kingman

Pilot scale microwave sorting of porphyry copper ores: Part 1 – Laboratory investigations

Miner. Eng., 98 (2016), pp. 303-327

View PDF View article View in Scopus ↗ Google Scholar ↗

Bluhm, 2006 H. Bluhm

Pulsed Power Systems

Springer, Berlin Heidelberg (2006)

Google Scholar ↗

Calvo et al., 2016 G. Calvo, G. Mudd, A. Valero, A. Valero

Decreasing Ore Grades in Global Metallic Mining: A Theoretical Issue or a Global Reality?

Resources, 5 (4) (2016), p. 36

CrossRef ↗ View in Scopus ↗ Google Scholar ↗

Cho et al., 2016 S.H. Cho, S.S. Cheong, M. Yokota, K. Kaneko

The Dynamic Fracture Process in Rocks Under High-Voltage Pulse Fragmentation

Rock Mech. Rock Eng., 49 (10) (2016), pp. 3841-3853

CrossRef ↗ View in Scopus ↗ Google Scholar ↗

Han et al., 2015 Han, Y., Liu, Y., Lin, F., Li, Z., Luo, Q., 2015. Experimental investigation of arc formation and bubble expansion initiated by pulse discharge in water. In: 2015 IEEE Pulsed Power Conference (PPC).

Google Scholar ↗

Huang, 2019 W. Huang

Selective Breakage of Mineralised Particles by High Voltage Pulses

University of Queensland (2019)

Google Scholar ↗

Huang et al., 2019 W. Huang, F. Ren, F. Shi, K. Steel

X-ray CT observations of selective damage of mineralised synthetic particles by high voltage pulses

Miner. Eng., 143 (2019)

Google Scholar ↗

Huang et al., 2020 W. Huang, F. Shi, C. Antonio, K. Runge

Influence of grade heterogeneity and gangue mineralogy on the efficacy of high voltage pulse enabled ore pre-concentration

Miner. Eng., 159 (2020), Article 106654

View PDF View article View in Scopus ↗ Google Scholar ↗

Mezzetti et al., 2018 M. Mezzetti, O. Popov, H. Lieberwirth, E. Anders, M. Voigt, P. Hoske

Microstructural investigation of complex ores processed with electric impulses

XXIX IMPC, Moscow, Russia (2018)

Google Scholar ↗

Mudd, 2007 G.M. Mudd

An assessment of the sustainability of the mining industry in Australia

Australian J. Multi-Disciplinary Eng., 5 (1) (2007), pp. 1-12

CrossRef ↗ View in Scopus ↗ Google Scholar ↗

Olhoeft, 1979 Olhoeft, G.R., 1979. Tables of room temperature electrical properties for selected rocks and minerals with dielectric permittivity statistics, US Department of the Interior Geological Survey open file report.

Google Scholar ↗

Shi and Manlapig, 2018 Shi, F., Manlapig, E., 2018. An integrated separator system and process for preconcentration and pretreatment of a material. International patent WO 2018/232438 A1.

Google Scholar ↗

Shi et al., 2013 F. Shi, W. Zuo, E. Manlapig

Characterisation of pre-weakening effect on ores by high voltage electrical pulses based on single-particle tests

Miner. Eng., 50–51 (2013), pp. 69-76

View PDF View article View in Scopus ↗ Google Scholar ↗

Usov and Tsukerman, 2002 Usov, A.F., Tsukerman, V.A., 2002. Prospective Electric Pulse Processes for Sustainable Processing of Mineral Raw Materials. International Conference on the Sustainable Processing of Minerals, Cairns, QLD.

Google Scholar ↗

Usov and Tsukerman, 2008 A. Usov, V. Tsukerman

Electric Pulse Disintegration: Russian Experience and Prospects

Rewas 2008: Global Symposium on Recycling, Waste Treatment and Clean Technology; Proceedings, John Wiley & Sons Inc: (2008), pp. 221-226

View in Scopus ↗ Google Scholar ↗

van der Wielen, 2013 K.P. van der Wielen

Application of High Voltage Breakage to a Range of Rock Types of Varying Physical Properties

University of Exeter (2013)

Google Scholar ↗

Voigt et al., 2020 Voigt, M., Anders, E., Lehmann, F., Mezzetti, M., Will, F., 2020. Electric Impulse Technology – Breaking Rock. In: 2020 22nd European Conference on Power Electronics and Applications. Lyon, France: 1-10.

Google Scholar ↗

Wang et al., 2011 E. Wang, F. Shi, E. Manlapig

Pre-weakening of mineral ores by high voltage pulses

Miner. Eng., 24 (5) (2011), pp. 455-462

View PDF View article View in Scopus ↗ Google Scholar ↗

Wang et al., 2012 E. Wang, F. Shi, E. Manlapig

Mineral liberation by high voltage pulses and conventional comminution with same specific energy levels

Miner. Eng., 27–28 (2012), pp. 28-36

View PDF View article View in Scopus ↗ Google Scholar ↗

Zuo et al., 2014 W. Zuo, F. Shi, E. Manlapig

Electrical breakdown channel locality in high voltage pulse breakage

Miner. Eng., 69 (2014), pp. 196-204

View PDF View article View in Scopus ↗ Google Scholar ↗

Zuo et al., 2015a W. Zuo, F. Shi, E. Manlapig

Pre-concentration of copper ores by high voltage pulses. Part 1: Principle and major findings

Miner. Eng., 79 (2015), pp. 306-314

View PDF View article View in Scopus ↗ Google Scholar ↗

Zuo et al., 2015b W. Zuo, F. Shi, K.P. van der Wielen, A. Weh

Ore particle breakage behaviour in a pilot scale high voltage pulse machine

Miner. Eng., 84 (2015), pp. 64-73

View PDF View article View in Scopus ↗ Google Scholar ↗

Cited by (1)

Mechanism and research progress of plasma induced cracking and enhancement in low permeability and hard to extract coal seams ↗

2023, Zhongguo Kuangye Daxue Xuebao/Journal of China University of Mining and Technology